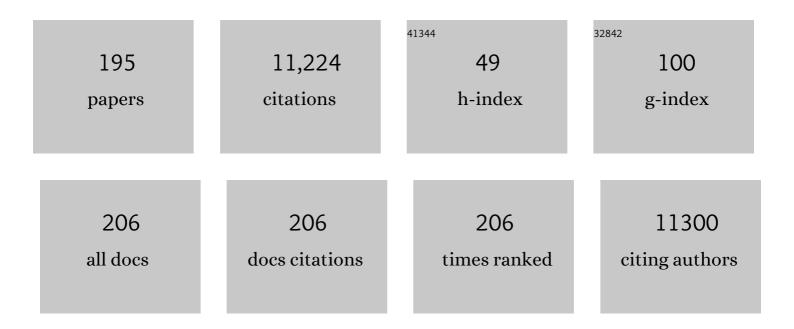


List of Publications by Year in descending order

Source: https://exaly.com/author-pdf/8672337/publications.pdf Version: 2024-02-01



I E VII

#	Article	IF	CITATIONS
1	Nighttime lights, urban features, household poverty, depression, and obesity. Current Psychology, 2023, 42, 15453-15464.	2.8	5
2	A study of the serious conflicts between oil palm expansion and biodiversity conservation using high-resolution remote sensing. Remote Sensing Letters, 2023, 14, 654-668.	1.4	0
3	A CNN-Based Self-Supervised Synthetic Aperture Radar Image Denoising Approach. IEEE Transactions on Geoscience and Remote Sensing, 2022, 60, 1-15.	6.3	10
4	Multisource-Domain Generalization-Based Oil Palm Tree Detection Using Very-High-Resolution (VHR) Satellite Images. IEEE Geoscience and Remote Sensing Letters, 2022, 19, 1-5.	3.1	5
5	The divergent response of vegetation phenology to urbanization: A case study of Beijing city, China. Science of the Total Environment, 2022, 803, 150079.	8.0	30
6	A fine-resolution estimation of the biomass resource potential across China from 2020 to 2100. Resources, Conservation and Recycling, 2022, 176, 105944.	10.8	19
7	Global urbanicity is associated with brain and behaviour in young people. Nature Human Behaviour, 2022, 6, 279-293.	12.0	24
8	Assessing spatiotemporal variations and predicting changes in ecosystem service values in the Guangdong–Hong Kong–Macao Greater Bay Area. GlScience and Remote Sensing, 2022, 59, 184-199.	5.9	21
9	The Accuracy of Winter Wheat Identification at Different Growth Stages Using Remote Sensing. Remote Sensing, 2022, 14, 893.	4.0	8
10	Sustainable Development Goals (SDGs) Priorities of Senior High School Students and Global Public: Recommendations for Implementing Education for Sustainable Development (ESD). Education Research International, 2022, 2022, 1-14.	1.1	6
11	Mapping spatial-temporal nationwide soybean planting area in Argentina using Google Earth Engine. International Journal of Remote Sensing, 2022, 43, 1724-1748.	2.9	5
12	A global map of planting years of plantations. Scientific Data, 2022, 9, 141.	5.3	24
13	Distribution of ecological restoration projects associated with land use and land cover change in China and their ecological impacts. Science of the Total Environment, 2022, 825, 153938.	8.0	56
14	Recent expansion of oil palm plantations into carbon-rich forests. Nature Sustainability, 2022, 5, 574-577.	23.7	14
15	An Overview of the Applications of Earth Observation Satellite Data: Impacts and Future Trends. Remote Sensing, 2022, 14, 1863.	4.0	61
16	Soybean EOS Spatiotemporal Characteristics and Their Climate Drivers in Global Major Regions. Remote Sensing, 2022, 14, 1867.	4.0	1
17	Contrasting influences of biogeophysical and biogeochemical impacts of historical land use on global economic inequality. Nature Communications, 2022, 13, 2479.	12.8	16
18	Characteristics of Greening along Altitudinal Gradients on the Qinghai–Tibet Plateau Based on Time-Series Landsat Images. Remote Sensing, 2022, 14, 2408.	4.0	11

#	Article	IF	CITATIONS
19	Global relative ecosystem service budget mapping using the Google Earth Engine and land cover datasets. Environmental Research Communications, 2022, 4, 065002.	2.3	2
20	ldentifying ecosystem service value and potential loss of wilderness areas in China to support post-2020 global biodiversity conservation. Science of the Total Environment, 2022, 846, 157348.	8.0	15
21	FROM-GLC Plus: toward near real-time and multi-resolution land cover mapping. GIScience and Remote Sensing, 2022, 59, 1026-1047.	5.9	29
22	How does urban expansion interact with cropland loss? A comparison of 14 Chinese cities from 1980 to 2015. Landscape Ecology, 2021, 36, 243-263.	4.2	62
23	The 2020 China report of the Lancet Countdown on health and climate change. Lancet Public Health, The, 2021, 6, e64-e81.	10.0	106
24	Harnessing synthetic biology-based strategies for engineered biosynthesis of nucleoside natural products in actinobacteria. Biotechnology Advances, 2021, 46, 107673.	11.7	8
25	Investigation of land surface phenology detections in shrublands using multiple scale satellite data. Remote Sensing of Environment, 2021, 252, 112133.	11.0	35
26	Livestock farmers' perception and adaptation to climate change: panel evidence from pastoral areas in China. Climatic Change, 2021, 164, 1.	3.6	7
27	Abnormal phosphorylation of tau protein and neuroinflammation induced by laparotomy in an animal model of postoperative delirium. Experimental Brain Research, 2021, 239, 867-880.	1.5	9
28	Climate response to introduction of the ESA CCI land cover data to the NCAR CESM. Climate Dynamics, 2021, 56, 4109-4127.	3.8	11
29	Significant Land Contributions to Interannual Predictability of East Asian Summer Monsoon Rainfall. Earth's Future, 2021, 9, e2020EF001762.	6.3	18
30	Growing status observation for oil palm trees using Unmanned Aerial Vehicle (UAV) images. ISPRS Journal of Photogrammetry and Remote Sensing, 2021, 173, 95-121.	11.1	91
31	Evaluation of Future Impacts of Climate Change, CO2, and Land Use Cover Change on Global Net Primary Productivity Using a Processed Model. Land, 2021, 10, 365.	2.9	5
32	A 30 m terrace mapping in China using Landsat 8 imagery and digital elevation model based on the Google Earth Engine. Earth System Science Data, 2021, 13, 2437-2456.	9.9	39
33	Mapping the maximum extents of urban green spaces in 1039 cities using dense satellite images. Environmental Research Letters, 2021, 16, 064072.	5.2	32
34	Fire enhances forest degradation within forest edge zones in Africa. Nature Geoscience, 2021, 14, 479-483.	12.9	26
35	Identifying Potential Cropland Losses When Conserving 30% and 50% Earth with Different Approaches and Spatial Scales. Land, 2021, 10, 704.	2.9	3
36	Oil palm modelling in the global land surface model ORCHIDEE-MICT. Geoscientific Model Development, 2021, 14, 4573-4592.	3.6	1

#	Article	IF	CITATIONS
37	Towards an open and synergistic framework for mapping global land cover. PeerJ, 2021, 9, e11877.	2.0	7
38	A large-scale, long time-series (1984‒2020) of soybean mapping with phenological features: Heilongjiang Province as a test case. International Journal of Remote Sensing, 2021, 42, 7332-7356.	2.9	8
39	Awareness of Sustainable Development Goals among Students from a Chinese Senior High School. Education Sciences, 2021, 11, 458.	2.6	24
40	The land footprint of the global food trade: Perspectives from a case study of soybeans. Land Use Policy, 2021, 111, 105764.	5.6	17
41	Progress and Trends in the Application of Google Earth and Google Earth Engine. Remote Sensing, 2021, 13, 3778.	4.0	71
42	Quantization of the coupling mechanism between eco-environmental quality and urbanization from multisource remote sensing data. Journal of Cleaner Production, 2021, 321, 128948.	9.3	98
43	One-third of lands face high conflict risk between biodiversity conservation and human activities in China. Journal of Environmental Management, 2021, 299, 113449.	7.8	21
44	Coconut Trees Detection on the Tenarunga Using High-Resolution Satellite Images and Deep Learning. , 2021, , .		5
45	Accuracy comparison and driving factor analysis of LULC changes using multi-source time-series remote sensing data in a coastal area. Ecological Informatics, 2021, 66, 101457.	5.2	9
46	Evaluating the Farmland Use Intensity and Its Patterns in a Farming—Pastoral Ecotone of Northern China. Remote Sensing, 2021, 13, 4304.	4.0	1
47	Annual dynamic dataset of global cropping intensity from 2001 to 2019. Scientific Data, 2021, 8, 283.	5.3	24
48	The 2021 China report of the Lancet Countdown on health and climate change: seizing the window of opportunity. Lancet Public Health, The, 2021, 6, e932-e947.	10.0	41
49	A 1 km global cropland dataset from 10 000 BCE to 2100 CE. Earth System Science Data, 202	21,919,54	03- 5 &121.
50	Efficient biosynthesis of nucleoside cytokinin angustmycin A containing an unusual sugar system. Nature Communications, 2021, 12, 6633.	12.8	12
51	Global Change of Land-Sparing and Land-Sharing Patterns over the Past 30 Years: Evidence from Remote Sensing and Statistics. Remote Sensing, 2021, 13, 5090.	4.0	0
52	Coupled modelling and sampling approaches to assess the impacts of human water management on land-sea carbon transfer. Science of the Total Environment, 2020, 701, 134735.	8.0	3
53	Oil palm plantation mapping from high-resolution remote sensing images using deep learning. International Journal of Remote Sensing, 2020, 41, 2022-2046.	2.9	25
54	Carbonaceous aerosol emission reduction over Shandong province and the impact of air pollution control as observed from synthetic satellite data. Atmospheric Environment, 2020, 222, 117150.	4.1	12

#	Article	IF	CITATIONS
55	Integrating Google Earth imagery with Landsat data to improve 30-m resolution land cover mapping. Remote Sensing of Environment, 2020, 237, 111563.	11.0	79
56	Monitoring Crop Growth During the Period of the Rapid Spread of COVID-19 in China by Remote Sensing. IEEE Journal of Selected Topics in Applied Earth Observations and Remote Sensing, 2020, 13, 6195-6205.	4.9	17
57	Cross-regional oil palm tree counting and detection via a multi-level attention domain adaptation network. ISPRS Journal of Photogrammetry and Remote Sensing, 2020, 167, 154-177.	11.1	51
58	Cross-Regional Oil Palm Tree Detection. , 2020, , .		10
59	Reducing human pressure on farmland could rescue China's declining wintering geese. Movement Ecology, 2020, 8, 35.	2.8	6
60	Exploring difference in land surface temperature between the city centres and urban expansion areas of China's major cities. International Journal of Remote Sensing, 2020, 41, 8965-8985.	2.9	13
61	Improved Mapping Results of 10 m Resolution Land Cover Classification in Guangdong, China Using Multisource Remote Sensing Data With Google Earth Engine. IEEE Journal of Selected Topics in Applied Earth Observations and Remote Sensing, 2020, 13, 5384-5397.	4.9	15
62	Synergy of Active and Passive Remote Sensing Data for Effective Mapping of Oil Palm Plantation in Malaysia. Forests, 2020, 11, 858.	2.1	17
63	Contrasting Effects of Temperature and Precipitation on Vegetation Greenness along Elevation Gradients of the Tibetan Plateau. Remote Sensing, 2020, 12, 2751.	4.0	29
64	Cost-effective priorities for the expansion of global terrestrial protected areas: Setting post-2020 global and national targets. Science Advances, 2020, 6, .	10.3	76
65	Exploring Annual Urban Expansions in the Guangdong-Hong Kong-Macau Greater Bay Area: Spatiotemporal Features and Driving Factors in 1986–2017. Remote Sensing, 2020, 12, 2615.	4.0	39
66	Improving 3-m Resolution Land Cover Mapping through Efficient Learning from an Imperfect 10-m Resolution Map. Remote Sensing, 2020, 12, 1418.	4.0	14
67	Mapping global urban boundaries from the global artificial impervious area (GAIA) data. Environmental Research Letters, 2020, 15, 094044.	5.2	240
68	Spatial distribution of usable biomass feedstock and technical bioenergy potential in China. GCB Bioenergy, 2020, 12, 54-70.	5.6	27
69	Annual 30-m land use/land cover maps of China for 1980–2015 from the integration of AVHRR, MODIS and Landsat data using the BFAST algorithm. Science China Earth Sciences, 2020, 63, 1390-1407.	5.2	64
70	Annual oil palm plantation maps in Malaysia and Indonesia from 2001 to 2016. Earth System Science Data, 2020, 12, 847-867.	9.9	50
71	Cropland heterogeneity changes on the Northeast China Plain in the last three decades (1980s–2010s). Peerl, 2020, 8, e9835.	2.0	2
72	Urban-Expansion Driven Farmland Loss Follows with the Environmental Kuznets Curve Hypothesis: Evidence from Temporal Analysis in Beijing, China. Communications in Computer and Information Science, 2020, , 394-412.	0.5	0

#	Article	IF	CITATIONS
73	Domain adversarial neural network-based oil palm detection using high-resolution satellite images. , 2020, , .		2
74	Jujubecake: An Extension of LSTM Considering Correlation among Input Blocks. , 2020, , .		1
75	The spatial-temporal patterns of land cover changes due to mining activities in the Darling Range, Western Australia: A Visual Analytics Approach. Ore Geology Reviews, 2019, 108, 23-32.	2.7	18
76	Spatial-temporal patterns of features selected using random forests: a case study of corn and soybeans mapping in the US. International Journal of Remote Sensing, 2019, 40, 269-283.	2.9	14
77	An Integrated Land Cover Mapping Method Suitable for Low-Accuracy Areas in Global Land Cover Maps. Remote Sensing, 2019, 11, 1777.	4.0	3
78	Analyzing land use intensity changes within and outside protected areas using ESA CCI-LC datasets. Global Ecology and Conservation, 2019, 20, e00789.	2.1	15
79	Estimating the Aboveground Biomass for Planted Forests Based on Stand Age and Environmental Variables. Remote Sensing, 2019, 11, 2270.	4.0	17
80	Exploring the addition of Landsat 8 thermal band in land-cover mapping. International Journal of Remote Sensing, 2019, 40, 4544-4559.	2.9	5
81	A Real-Time Tree Crown Detection Approach for Large-Scale Remote Sensing Images on FPGAs. Remote Sensing, 2019, 11, 1025.	4.0	23
82	Oxygen vacancy-enriched MoO _{3â^'x} nanobelts for asymmetric supercapacitors with excellent room/low temperature performance. Journal of Materials Chemistry A, 2019, 7, 13205-13214.	10.3	92
83	A structured approach to the analysis of remote sensing images. International Journal of Remote Sensing, 2019, 40, 7874-7897.	2.9	2
84	Managing nitrogen to restore water quality in China. Nature, 2019, 567, 516-520.	27.8	667
85	Stable classification with limited sample: transferring a 30-m resolution sample set collected in 2015 to mapping 10-m resolution global land cover in 2017. Science Bulletin, 2019, 64, 370-373.	9.0	761
86	Design of multiple electrode structures based on nano Ni ₃ S ₂ and carbon nanotubes for high performance supercapacitors. Journal of Materials Chemistry A, 2019, 7, 7406-7414.	10.3	45
87	Comparisons of three recent moderate resolution African land cover datasets: CGLS-LC100, ESA-S2-LC20, and FROM-GLC-Africa30. International Journal of Remote Sensing, 2019, 40, 6185-6202.	2.9	43
88	Long-Term Land Cover Dynamics (1986–2016) of Northeast China Derived from a Multi-Temporal Landsat Archive. Remote Sensing, 2019, 11, 599.	4.0	35
89	Mapping oil palm plantation expansion in Malaysia over the past decade (2007–2016) using ALOS-1/2 PALSAR-1/2 data. International Journal of Remote Sensing, 2019, 40, 7389-7408.	2.9	17
90	Semantic Segmentation-Based Building Footprint Extraction Using Very High-Resolution Satellite Images and Multi-Source GIS Data. Remote Sensing, 2019, 11, 403.	4.0	135

#	Article	IF	CITATIONS
91	Assessment of the potential and distribution of an energy crop at 1-km resolution from 2010 to 2100 in China – The case of sweet sorghum. Applied Energy, 2019, 239, 395-407.	10.1	18
92	High resolution crop intensity mapping using harmonized Landsat-8 and Sentinel-2 data. Journal of Integrative Agriculture, 2019, 18, 2883-2897.	3.5	40
93	Global urban expansion offsets climate-driven increases in terrestrial net primary productivity. Nature Communications, 2019, 10, 5558.	12.8	198
94	Spatiotemporal crop NDVI responses to climatic factors in mainland China. International Journal of Remote Sensing, 2019, 40, 89-103.	2.9	6
95	Large-Scale Oil Palm Tree Detection from High-Resolution Satellite Images Using Two-Stage Convolutional Neural Networks. Remote Sensing, 2019, 11, 11.	4.0	93
96	Precision medicine and global mental health. The Lancet Global Health, 2019, 7, e32.	6.3	21
97	Matching area selection of an underwater terrain navigation database with fuzzy multi-attribute decision making method. Proceedings of the Institution of Mechanical Engineers Part M: Journal of Engineering for the Maritime Environment, 2019, 233, 1133-1140.	0.5	2
98	Semantic segmentation based large-scale oil palm plantation detection using high-resolution satellite images. , 2019, , .		4
99	Fast and robust detection of oil palm trees using high-resolution remote sensing images. , 2019, , .		7
100	Assessing the Impacts of Extreme Agricultural Droughts in China Under Climate and Socioeconomic Changes. Earth's Future, 2018, 6, 689-703.	6.3	72
101	Comparison of country-level cropland areas between ESA-CCI land cover maps and FAOSTAT data. International Journal of Remote Sensing, 2018, 39, 6631-6645.	2.9	49
102	Multi-scale habitat selection by two declining East Asian waterfowl species at their core spring stopover area. Ecological Indicators, 2018, 87, 127-135.	6.3	34
103	Difficult to map regions in 30 m global land cover mapping determined with a common validation dataset. International Journal of Remote Sensing, 2018, 39, 4077-4087.	2.9	14
104	Scaling up spring phenology derived from remote sensing images. Agricultural and Forest Meteorology, 2018, 256-257, 207-219.	4.8	21
105	A multiple dataset approach for 30-m resolution land cover mapping: a case study of continental Africa. International Journal of Remote Sensing, 2018, 39, 3926-3938.	2.9	25
106	Mapping oil palm extent in Malaysia using ALOS-2 PALSAR-2 data. International Journal of Remote Sensing, 2018, 39, 432-452.	2.9	26
107	Mineral composition of the Martian Gale and Nili Fossae regions from Mars Reconnaissance Orbiter CRISM images. Planetary and Space Science, 2018, 163, 97-105.	1.7	6
108	Tracking annual cropland changes from 1984 to 2016 using time-series Landsat images with a change-detection and post-classification approach: Experiments from three sites in Africa. Remote Sensing of Environment, 2018, 218, 13-31.	11.0	71

#	Article	IF	CITATIONS
109	A sampling workflow based on unsupervised clusters and multi-temporal sample interpretation (UCMT) for cropland mapping. Remote Sensing Letters, 2018, 9, 952-961.	1.4	2
110	Assessing spectral indices to estimate the fraction of photosynthetically active radiation absorbed by the vegetation canopy. International Journal of Remote Sensing, 2018, 39, 8022-8040.	2.9	17
111	Long-Term Annual Mapping of Four Cities on Different Continents by Applying a Deep Information Learning Method to Landsat Data. Remote Sensing, 2018, 10, 471.	4.0	50
112	The Evaluation of SMAP Enhanced Soil Moisture Products Using High-Resolution Model Simulations and In-Situ Observations on the Tibetan Plateau. Remote Sensing, 2018, 10, 535.	4.0	37
113	Towards global oil palm plantation mapping using remote-sensing data. International Journal of Remote Sensing, 2018, 39, 5891-5906.	2.9	23
114	Comparison of the Spatial Characteristics of Four Remotely Sensed Leaf Area Index Products over China: Direct Validation and Relative Uncertainties. Remote Sensing, 2018, 10, 148.	4.0	35
115	Identifying patterns and hotspots of global land cover transitions using the ESA CCI Land Cover dataset. Remote Sensing Letters, 2018, 9, 972-981.	1.4	63
116	Monitoring surface mining belts using multiple remote sensing datasets: A global perspective. Ore Geology Reviews, 2018, 101, 675-687.	2.7	40
117	Wrapping RGO/MoO2/carbon textile as supercapacitor electrode with enhanced flexibility and areal capacitance. Electrochimica Acta, 2018, 282, 784-791.	5.2	20
118	Exploring the temporal density of Landsat observations for cropland mapping: experiments from Egypt, Ethiopia, and South Africa. International Journal of Remote Sensing, 2018, 39, 7328-7349.	2.9	7
119	Using a global reference sample set and a cropland map for area estimation in China. Science China Earth Sciences, 2017, 60, 277-285.	5.2	18
120	Assessment of the cropland classifications in four global land cover datasets: A case study of Shaanxi Province, China. Journal of Integrative Agriculture, 2017, 16, 298-311.	3.5	23
121	Coordination Polymers Derived General Synthesis of Multishelled Mixed Metalâ€Oxide Particles for Hybrid Supercapacitors. Advanced Materials, 2017, 29, 1605902.	21.0	345
122	Towards a global oil palm sample database: design and implications. International Journal of Remote Sensing, 2017, 38, 4022-4032.	2.9	15
123	Exploring the correlations between ten monthly climatic variables and the vegetation index of four different crop types at the global scale. Remote Sensing Letters, 2017, 8, 752-760.	1.4	3
124	Mapping finerâ€resolution land surface emissivity using Landsat images in China. Journal of Geophysical Research D: Atmospheres, 2017, 122, 6764-6781.	3.3	34
125	Monitoring cropland changes along the Nile River in Egypt over past three decades (1984–2015) using remote sensing. International Journal of Remote Sensing, 2017, 38, 4459-4480.	2.9	27
126	The first all-season sample set for mapping global land cover with Landsat-8 data. Science Bulletin, 2017, 62, 508-515.	9.0	104

#	Article	IF	CITATIONS
127	Exploring the performance of spatio-temporal assimilation in an urban cellular automata model. International Journal of Geographical Information Science, 2017, 31, 2195-2215.	4.8	5
128	On the Growth and Detectability of Land Plants on Habitable Planets around M Dwarfs. Astrobiology, 2017, 17, 1219-1232.	3.0	4
129	A segment derived patch-based logistic cellular automata for urban growth modeling with heuristic rules. Computers, Environment and Urban Systems, 2017, 65, 140-149.	7.1	53
130	A multiple crop model ensemble for improving broad-scale yield prediction using Bayesian model averaging. Field Crops Research, 2017, 211, 114-124.	5.1	39
131	Parallel Multiclass Support Vector Machine for Remote Sensing Data Classification on Multicore and Many-Core Architectures. IEEE Journal of Selected Topics in Applied Earth Observations and Remote Sensing, 2017, 10, 4387-4398.	4.9	13
132	Formation of Onion‣ike NiCo ₂ S ₄ Particles via Sequential Ionâ€Exchange for Hybrid Supercapacitors. Advanced Materials, 2017, 29, 1605051.	21.0	539
133	Deep convolutional neural network based large-scale oil palm tree detection for high-resolution remote sensing images. , 2017, , .		17
134	Deep Learning Based Oil Palm Tree Detection and Counting for High-Resolution Remote Sensing Images. Remote Sensing, 2017, 9, 22.	4.0	284
135	Assessing and Improving the Reliability of Volunteered Land Cover Reference Data. Remote Sensing, 2017, 9, 1034.	4.0	9
136	High Resolution Mapping of Cropping Cycles by Fusion of Landsat and MODIS Data. Remote Sensing, 2017, 9, 1232.	4.0	20
137	Evaluation of the Common Land Model (CoLM) from the Perspective of Water and Energy Budget Simulation: Towards Inclusion in CMIP6. Atmosphere, 2017, 8, 141.	2.3	18
138	Green Spaces as an Indicator of Urban Health: Evaluating Its Changes in 28 Mega-Cities. Remote Sensing, 2017, 9, 1266.	4.0	67
139	Long-Term Post-Disturbance Forest Recovery in the Greater Yellowstone Ecosystem Analyzed Using Landsat Time Series Stack. Remote Sensing, 2016, 8, 898.	4.0	37
140	Analysis and Simulation of Geomagnetic Map Suitability Based on Vague Set. Journal of Navigation, 2016, 69, 1114-1124.	1.7	9
141	Rapid corn and soybean mapping in US Corn Belt and neighboring areas. Scientific Reports, 2016, 6, 36240.	3.3	38
142	A new research paradigm for global land cover mapping. Annals of GIS, 2016, 22, 87-102.	3.1	77
143	Ten years after Hurricane Katrina: monitoring recovery in New Orleans and the surrounding areas using remote sensing. Science Bulletin, 2016, 61, 1460-1470.	9.0	20
144	Climate effects of the GlobeLand30 land cover dataset on the Beijing Climate Center climate model simulations. Science China Earth Sciences, 2016, 59, 1754-1764.	5.2	14

#	Article	IF	CITATIONS
145	An all-season sample database for improving land-cover mapping of Africa with two classification schemes. International Journal of Remote Sensing, 2016, 37, 4623-4647.	2.9	24
146	Circa 2014 African land-cover maps compatible with FROM-GLC and GLC2000 classification schemes based on multi-seasonal Landsat data. International Journal of Remote Sensing, 2016, 37, 4648-4664.	2.9	25
147	A cellular automata downscaling based 1 km global land use datasets (2010–2100). Science Bulletin, 2016, 61, 1651-1661.	9.0	68
148	A Fully Automatic Method to Extract Rare Earth Mining Areas from Landsat Images. Photogrammetric Engineering and Remote Sensing, 2016, 82, 729-737.	0.6	8
149	Automated mapping of soybean and corn using phenology. ISPRS Journal of Photogrammetry and Remote Sensing, 2016, 119, 151-164.	11.1	156
150	Stacked Autoencoder-based deep learning for remote-sensing image classification: a case study of African land-cover mapping. International Journal of Remote Sensing, 2016, 37, 5632-5646.	2.9	142
151	Exploring the potential role of feature selection in global land-cover mapping. International Journal of Remote Sensing, 2016, 37, 5491-5504.	2.9	14
152	Oil palm mapping using Landsat and PALSAR: a case study in Malaysia. International Journal of Remote Sensing, 2016, 37, 5431-5442.	2.9	41
153	Detailed dynamic land cover mapping of Chile: Accuracy improvement by integrating multi-temporal data. Remote Sensing of Environment, 2016, 183, 170-185.	11.0	146
154	Land cover mapping and data availability in critical terrestrial ecoregions: A global perspective with Landsat thematic mapper and enhanced thematic mapper plus data. Biological Conservation, 2015, 190, 34-42.	4.1	33
155	Construction Method of the Topographical Features Model for Underwater Terrain Navigation. Polish Maritime Research, 2015, 22, 121-125.	1.9	8
156	Geographic stacking: Decision fusion to increase global land cover map accuracy. ISPRS Journal of Photogrammetry and Remote Sensing, 2015, 103, 57-65.	11.1	38
157	A generalization of spatial and temporal fusion methods for remotely sensed surface parameters. International Journal of Remote Sensing, 2015, 36, 4411-4445.	2.9	56
158	Multi-scale evaluation of light use efficiency in MODIS gross primary productivity for croplands in the Midwestern United States. Agricultural and Forest Meteorology, 2015, 201, 111-119.	4.8	51
159	Mapping global land cover in 2001 and 2010 with spatial-temporal consistency at 250m resolution. ISPRS Journal of Photogrammetry and Remote Sensing, 2015, 103, 38-47.	11.1	99
160	A Circa 2010 Thirty Meter Resolution Forest Map for China. Remote Sensing, 2014, 6, 5325-5343.	4.0	37
161	Global-Scale Associations of Vegetation Phenology with Rainfall and Temperature at a High Spatio-Temporal Resolution. Remote Sensing, 2014, 6, 7320-7338.	4.0	33
162	A 30 meter land cover mapping of China with an efficient clustering algorithm CBEST. Science China Earth Sciences, 2014, 57, 2293-2304.	5.2	18

#	Article	IF	CITATIONS
163	General Formation of MS (M = Ni, Cu, Mn) Boxâ€inâ€Box Hollow Structures with Enhanced Pseudocapacitive Properties. Advanced Functional Materials, 2014, 24, 7440-7446.	14.9	281
164	Variational model-based very high spatial resolution remote sensing image fusion. Journal of Applied Remote Sensing, 2014, 8, 083565.	1.3	2
165	A multi-resolution global land cover dataset through multisource data aggregation. Science China Earth Sciences, 2014, 57, 2317-2329.	5.2	116
166	A systematic sensitivity analysis of constrained cellular automata model for urban growth simulation based on different transition rules. International Journal of Geographical Information Science, 2014, 28, 1317-1335.	4.8	79
167	Intermodality models in pan-sharpening: analysis based on remote sensing physics. International Journal of Remote Sensing, 2014, 35, 515-531.	2.9	5
168	Towards a common validation sample set for global land-cover mapping. International Journal of Remote Sensing, 2014, 35, 4795-4814.	2.9	154
169	Meta-discoveries from a synthesis of satellite-based land-cover mapping research. International Journal of Remote Sensing, 2014, 35, 4573-4588.	2.9	130
170	Aggregative model-based classifier ensemble for improving land-use/cover classification of Landsat TM Images. International Journal of Remote Sensing, 2014, 35, 1481-1495.	2.9	23
171	FROM-GC: 30 m global cropland extent derived through multisource data integration. International Journal of Digital Earth, 2013, 6, 521-533.	3.9	123
172	Finer resolution observation and monitoring of global land cover: first mapping results with Landsat TM and ETM+ data. International Journal of Remote Sensing, 2013, 34, 2607-2654.	2.9	1,263
173	Improving 30Âm global land-cover map FROM-GLC with time series MODIS and auxiliary data sets: a segmentation-based approach. International Journal of Remote Sensing, 2013, 34, 5851-5867.	2.9	146
174	A Production Efficiency Model-Based Method for Satellite Estimates of Corn and Soybean Yields in the Midwestern US. Remote Sensing, 2013, 5, 5926-5943.	4.0	50
175	Towards the automatic selection of optimal seam line locations when merging optical remote-sensing images. International Journal of Remote Sensing, 2012, 33, 1000-1014.	2.9	45
176	Network Security Evaluation Model Based on Cloud Computing. Communications in Computer and Information Science, 2012, , 488-495.	0.5	1
177	Coogle Earth as a virtual globe tool for Earth science applications at the global scale: progress and perspectives. International Journal of Remote Sensing, 2012, 33, 3966-3986.	2.9	257
178	Towards automatic lithological classification from remote sensing data using support vector machines. Computers and Geosciences, 2012, 45, 229-239.	4.2	162
179	China's urban expansion from 1990 to 2010 determined with satellite remote sensing. Science Bulletin, 2012, 57, 2802-2812.	1.7	265
180	Improving Landsat ETM+ Urban Area Mapping via Spatial and Angular Fusion With MISR Multi-Angle Observations. IEEE Journal of Selected Topics in Applied Earth Observations and Remote Sensing, 2012, 5, 101-109.	4.9	22

#	Article	IF	CITATIONS
181	Spatial multi-objective land use optimization: extensions to the non-dominated sorting genetic algorithm-II. International Journal of Geographical Information Science, 2011, 25, 1949-1969.	4.8	176
182	A fast removal method of thin cloud/haze cover for optical remote sensing images based on multi-fractal. Proceedings of SPIE, 2011, , .	0.8	1
183	Suppression of vegetation in multispectral remote sensing images. International Journal of Remote Sensing, 2011, 32, 7343-7357.	2.9	14
184	Conjugate Gradient Method Neural Network for Medium Resolution Remote Sensing Image Classification. Communications in Computer and Information Science, 2011, , 264-270.	0.5	2
185	A study of PS-InSAR method for small area urban land subsidence. , 2010, , .		Ο
186	Mapping geochemical singularity using multifractal analysis: Application to anomaly definition on stream sediments data from Funin Sheet, Yunnan, China. Journal of Geochemical Exploration, 2010, 104, 1-11.	3.2	69
187	Forward XPath rewriting over XML data streams. , 2009, , .		Ο
188	A fast and fully automatic registration approach based on point features for multi-source remote-sensing images. Computers and Geosciences, 2008, 34, 838-848.	4.2	129
189	Open Geospatial Information Services Chaining Based on OGC Specifications and Processing Model. , 2008, , .		1
190	Monitoring Land Subsidence by Using Multi-temporal Differential SAR Interferometry: A Use Case in Jiaxing, China. , 2008, , .	_	0
191	A Standard Based Spatial Information Service Model for Adaptive Services Chaining. , 2008, , .		1
192	Characteristics of Remote Sensing Emission Spectra of Composite Igneous Rocks. , 2008, , .		2
193	Automatic registration for ASAR and TM images based on region features. , 2007, , .		2
194	Implementation of data node in spatial information grid based on WS resource framework and WS notification. , 2006, , .		0
195	Exploring intra-annual variation in cropland classification accuracy using monthly, seasonal, and yearly sample set. International Journal of Remote Sensing, 0, , 1-16.	2.9	7